Airborne Gamma-ray Spectrometry: Empirical Radon Correction

Eugene Druker
Geophysical Consultant, Canada

Abstract

In AGRS data processing, an important problem is the radon correction. This problem arises from the fact that the main emitters of the radioactive family U-238 are the same in the air and in the earth. Therefore, they cannot be distinguished by energies. However, without corrections for radon in the air, data on geological emitters can be distorted beyond recognition (overestimated many times). Several methods for radon correction are already known. They are based on special methods of radiation measurements or on a comparison of spectra from radiators of different energy. Their weak points are the need for complex calibrations and the need for powerful averaging in time and/or space, which completely contradicts the temporal and local character of the measured gamma fields. Here another radon correction is proposed, devoid of these shortcomings and having others. The correction is based on local features of the spectra near the photopeaks. In particular, it does not depend too much on accurate calibrations and is suitable not only for the standard energy of uranium at 1.76 MeV; on the other hand, it includes notable noises from measurements and calculations, which have to be handled in somewhat coarse ways.

Introduction

In the processing of AGRS data, one of the most difficult problems is a correction of the measured data for the effect of radon in the air. The problem is due to the fact that the main emitters of the U-238 family in the ground and in the air are the same. This section briefly discusses the main consequences of this phenomenon, some properties of gamma emitters in the air, known radon corrections and their features.

By tradition, word radon and symbol Rn will be used here as a common name for sources in the air and word uranium and symbol U as a common name for sources in the earth.

The main gamma-ray emitters of the U-238 family in the ground and in the air are the decay products of radon Rn-222, primarily the metals Pb-214 and Bi-214, therefore, the gamma spectra of sources in the earth and in the air are indistinguishable by energy, however only sources in the earth are of geological interest. Thus, the ability to separate sources in the ground and in the air, and, possibly, their spectra is required - this is called the radon correction. The effect of radon on AGRS data is diverse:

• in general, radon is closer to the gamma sensor than uranium and radon is located anywhere relative to the sensor - this creates a situation 4π measurement geometry

• radon is very mobile in air (wind, rain, temperature, etc.); the uniform distribution of radon in air is highly questionable and poorly related to the geology of the survey area

• radon just above the ground (up to 0.1 of flight altitude) cannot be distinguished from uranium just below the surface of the earth; this feature is exacerbated by influence of vegetation, water saturation, etc.

• significant levels of radon in the air can create gamma fields that greatly exceed the fields of uranium in the ground; radon products can fall to the ground and create temporary false anomalous fields (IAEA, 2013)

Some conclusions from this list are obvious:

• exhaustive, right and exact, radon correction is impossible

• it is impossible, after radon correction, to get the same spatial resolution for uranium as if there is no radon

• it is difficult to simulate the real influence of radon using Monte Carlo methods: the shape, location, intensity of the field sources are uncertain and may change during the measurements

• substantial averaging and/or smoothing of measurements is required to obtain worthwhile estimates.

One of the difficulties in the radon correction is that in the decay chain of uranium there is a gas radon Rn-222, which, during decay, gives the main gamma emitters of the U-238 uranium family. In the ground, they are almost immobile and are approximately in equilibrium with uranium and therefore can be used to assess uranium itself. In the air, radon behaves like a true gas, while its decay products are attached to aerosols and live by different rules, so usually there is no equilibrium between them, and often there are large deviations from equilibrium (Hotzl and Winkler, 1993). Moreover, their disequilibrium itself serves to study atmospheric processes. In general, radon has traditionally been used as the atmospheric tracer for studying air masses and their moving (Bristow, 1983; Chen et al., 2016).

Briefly consider the known methods for radon correction (IAEA, 2003; Killeen et al., 2015).

1. (Grasty et al., 1988; Grasty and Minty, 1995; IAEA, 1991)

An additional “upper” sensor is placed above the main sensor block. A special instrumental pulse counting system is recommended. This provides a 2π measurement geometry for the upper sensor. To apply this correction, a rather strong averaging of the measured data is required - it is recommended about 200 seconds for 32L down + 8L up; 600 are often used (Minty et al., 1997). The technical and methodological complexity of this correction arises from the desire to separate the sources of radiation into those located in the upper and lower half-spaces. The correction uses data of energy windows at 1.76 MeV.

2. (Minty, 1992; Minty, 1998)

These corrections are based on differences in attenuation Bi-214 photopeak at 0.609 MeV and its photopeak at 1.76 MeV. First correction uses energy windows of two peaks, second correction uses representation of the spectra as sum of four spectra (K, U, Th, and Rn). Quite strong, about 300 seconds, averaging is required. The calibration is described by Grasty and Minty (1995) and Minty et al. (1997). It is recommended to use the correction at altitudes over 100 m to avoid overlays with photopeak at 0.583 MeV. There is also a simplified version of this correction (Minty et al., 1998). The correction is not applicable in the presence of Cs-137, i.e. in the northern hemisphere (Minty et al., 1997), and there are a few more limitations. The correction uses multichannel data.

3. (Jurza et al., 2005)

This correction is based on the use of a photopeak of Pb-214 with an energy of 0.352 MeV. It is similar to the previous correction. The advantage is a slightly better peak selection of 0.352 MeV against the background of photopeaks of Th-232. Averaging up to 100 seconds or using the NASVD method is recommended (Hovgaard and Grasty, 1997). The correction uses multichannel data.

These corrections are intended to correct uranium in the energy window for 1.76 MeV. All corrections require several calibration flights under special conditions or several calibration pads; in particular, they are united by the certainty that calibration flights can be performed both in the presence and absence of radon. All corrections implicitly suggest a uniform distribution of radon in the lower atmosphere and still require quite powerful averaging of 200-600 seconds (IAEA, 2003) along survey lines or even ignoring time (NASVD); this, in general, means a serious, or even complete, loss of locality.

The various descriptions of the corrections do not contain an explicit and clear specification of the model of radon distribution in the air, although the proximity of radon to the sensor is usually mentioned and the uniform distribution of radon in air is implied. This situation, of course, is not an accident. Firstly, there is no reason to believe that the same model is true for each line and for the entire survey. A large averaging distance imposes a near-constant radon correction for the line or survey. Secondly, the air - the source of radon - also moves during the measurements, and at different times in different and unknown directions. Further, the assumed homogeneity of the distribution of radon in the air is exotic rather than rare situation. Apparently, a fairly good visual, albeit slightly poetic, idea of the distribution of radon in the air gives the sky with clouds or fog near the ground. Finally, corrections based on a comparison of the spectra (Bi-214 at 0.609 MeV and Pb-214 at 0.352 MeV) have computational difficulties due to the fact that in the peak region E of these energies, in the ranges (E-FWHM/2, E+FWHM/2), they intersect with 2-4 similar peaks of other emitters, including those from other families (FWHM is abbreviation for Full Width at Half Magnitude).

Here another correction is proposed, based on measurable statistical parameters of the spectra and the survey rather than on the features of the emitters and spectra, or on the assumptions about the distribution of radon. The main advantages of the proposed correction is its simplicity and locality.

Method

All data and considerations described in this section and further refer only to NaI(Tl) sensors made up of standard-sized 4"x4"x10" crystals. In surveys, only conventional sensors with volumes of 16L, 32L, and 48L, were used.

For large airborne gamma spectrometers, resolution R and energy E are related by good approximation (Druker, 2018):

$$E \cdot R^2(E) = \text{const.} \qquad (1)$$

The relation (1) will be used with the parameters E_0 = 0.662 MeV, $R_0(E_0)$ = 8.2%. The photopeak of each primary energy is approximated by a bell shape of the form $\text{bell}(\alpha,k) = \exp(-\alpha \cdot k^2)$, where $\alpha = \alpha(R)$, and the width of the photopeak, which determines the resolution at the central energy is $FWHM = R \cdot E = \sqrt{(\text{const} \cdot E)}$.

For several standard energies (IAEA, 1991), the corresponding parameters are given in Table 1, where known data is used (Grasty and Darnley, 1971; IAEA, 1979; IAEA, 2003).

Note that in all these cases the left edge of the window or band is to the right of the Compton edge, i.e. falls into the “multiple Compton scattering” area (Knoll, 2000).

Table 1. Standard energy windows and applied bands with ends at $\text{bell}(\alpha,k) = \delta \approx 0.01$. Energy in first column is used also as the band name, without word "MeV".

Energy, MeV	Element series	Standard window	Band range $\delta \approx 0.01$	Compton Edge
2.61	Th-232	2.41–2.81	2.48–2.75	2.38
1.76	U-238	1.66–1.86	1.65–1.88	1.54
1.46	K-40	1.37–1.57	1.36–1.57	1.24
1.12	U-238		1.03–1.21	0.91

Approximation (1) provides an opportunity to use triangles instead of bells, because photopeaks in Table 1 do not overlap. It is shown in Fig.1.

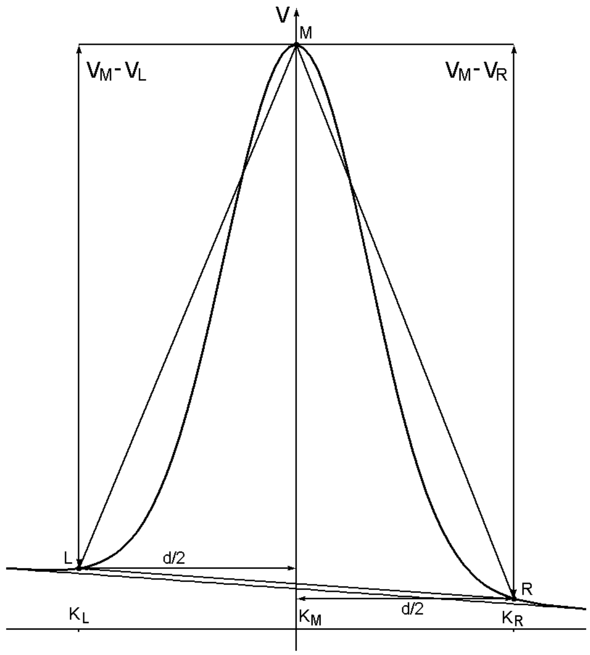

Fig. 1. Approximation the bell with the triangle. Thick line – bell (Gaussian curve). Horizontal axis – energy. Vertical axis – count rate.

The main points for calculations in Fig. 1 are L, M, and R, at energy channels K_L, K_M, and K_R - left, middle, right energy, $d/2 = K_R - K_M = K_M - K_L$. The count rates in these points are V_L, V_M, and V_R. The photopeak area is the area of a bell together with small tails, where bell $(\alpha, k) < \delta \approx 0.01$. This photopeak area corresponds to the area of the triangle LMR. It can be shown that under condition (1) between the area of the triangle A_T

$$A_T = (d/4)(2V_M - V_L - V_R) \qquad (2)$$

and the area of the bell A_B there is the approximate ratio

$$A_B = A_T \sqrt{(-\pi/\log(\delta))} = 0.826\ A_T, \qquad (3)$$

that does not depend on energy. The second parameter is dimensionless Skew:

$$S = (V_M - V_R)/(V_M - V_L). \qquad (4)$$

The survey chosen for illustration has qualities that make it suitable for the issues under consideration, although it is not as good as standard AGRS survey.

In the survey, there are about 122400 data points, 40 flights and 340 EW lines with 100 m nominal distance between them, with 360 data points on each line in average. The survey was flown in summertime in mountainous terrain in northern mid-latitudes.

Some maps are shown in Fig.2. In Fig.2(c), the air density map is a good indicator of survey flights.

Actual values in the flight lines are of somewhat wider range, than in Fig.2, that was decreased by gridding.

To make an averaging mentioned in introduction it is necessary to estimate the distances that ensure valid averaging within reasonable limits.

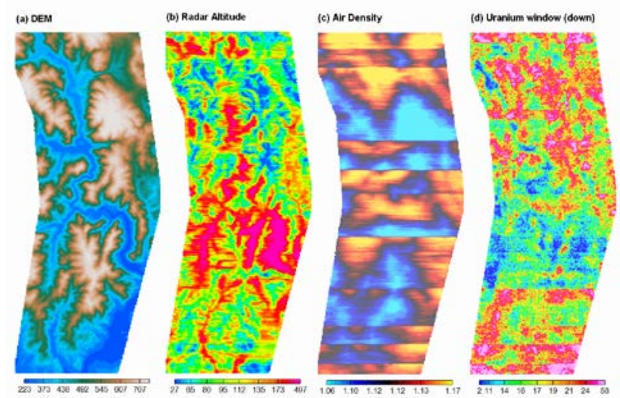

Fig. 2. Maps of AGRS survey, left to right: (a) DEM, m; (b) radar altitude, m; (c) air density, kg/m^3; (d) standard raw channel “uranium 1.76 down”, cps.

A simple estimate can be made from the linear attenuation coefficient μ. The reciprocal of the attenuation coefficient 1/μ has units of length and is called the mean free path, MFP. The MFP is the average distance a photon travels in the absorber before interacting; at this distance, the field attenuates by $e \approx 2.72$ times (Nelson and Reilly, 1990).

Table 2. MFP in air for typical energies (IAEA, 1979):

Energy, MeV	1.12	1.46	1.76	2.61
MFP, m	141	161	177	215

Table 3. Attenuation of gamma radiation for some MFP values:

No. of MFP	0	1	2	3	4
Attenuation	1.00	0.37	0.14	0.05	0.02

Thus, reasonable maximal distance of summation hardly exceeds 3 MFP, which means 10-20 seconds for helicopter speed of 30 m/s. A similar estimate is given by the model of a radiating-absorbing ball with a sensor at its center.

Both estimates give a similar result: the data at distances of more than 2–3 MFP should not be taken into account. For example, let MFP = 177 m and aircraft speed is 30 m/s. Then summation length for 3 MFP is about 3*177*2/30 = 35 seconds. Such a short filter cannot sufficiently suppress noises. By experience, it makes sense to apply several different filters and several options for summing adjacent channels. Typically, at 1.12, more than 75% of the points, and at 1.46, more than 95% of the points get values that have (some formal) meaning. Another possibility will be described below.

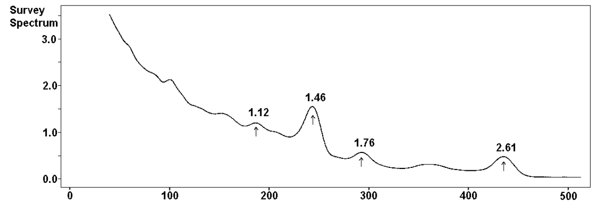

Fig. 3. Cumulative mean spectrum for the survey. Logarithmic scale for spectrum in 512 channels.

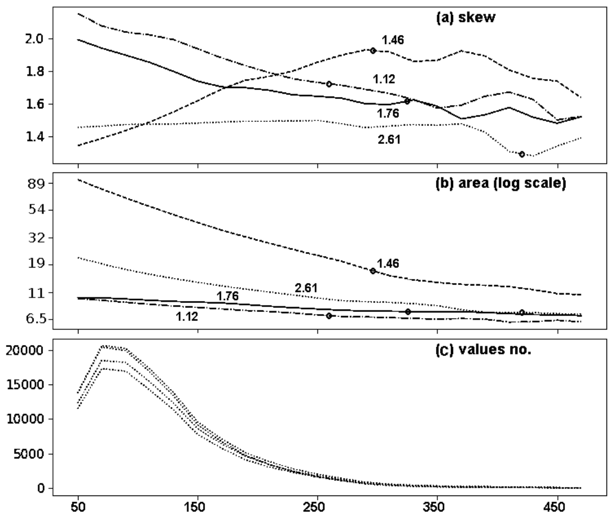

Fig. 4. Dependence of parameters on the flight height. Small circles on the curves mark heights of 2*MFP for values of energies and MFP from Table 2.

Skew in Fig.4a: Skew 2.61 does not change with height because there is no radon influence. Skew 1.12 and 1.76 are similar going down from 2-2.5 to 1.6. Skew 1.46 shows unclear behavior.

Area in Fig.4b: Areas 1.12 and 1.76 decrease much slower than 1.46 and 2.61. This is a sure sign of the presence of radon.

Values in Fig.4c: The number of data points is as follows: thousands up to heights of 250 m; hundreds up to heights of 350 m; tens for heights above 350 m – they do not characterize the area, but small spots.

Statistics show that Skew is a good candidate to participate in the radon correction. Consider it in more detail. Its definition is (4), the component values are shown in Fig. 1.

Further, for simplicity, instead of symbol Rn, it will be simply R. Schematically, the spectrum as a triangle in Fig.1 looks like in Fig.5. There are three triangles in Fig.5 for uranium U, radon R and their sum V.

For definiteness, consider 1.76. Suppose that on the right edge at E_2 there is no influence of either uranium or radon. Let E_0=1.66, E_1=1.76, E_2=1.86, d1=d2.

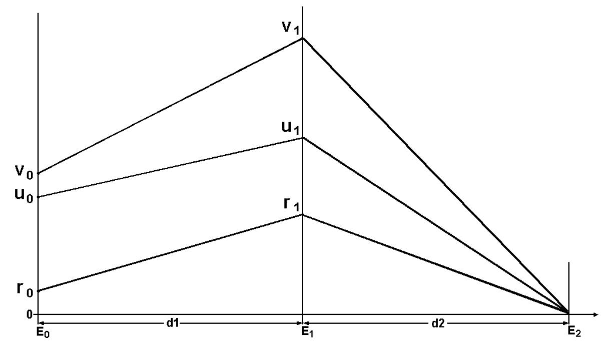

Fig. 5. Schematically, the triangles of photopeaks at 176.

Let A_U, A_R, and A_V – areas of U, R, and V triangles. Then the summation assumptions are written as

$$A_V = A_U + A_R,\ V_0 = R_0 + U_0,\ V_1 = R_1 + U_1. \qquad (5)$$

The parameters Skew defined in (4) now look like:

$$S_U=U_1/(U_1-U_0),\ S_R=R_1/(R_1-R_0),\ S_V=V_1/(V_1-V_0), \qquad (6)$$

Under these assumptions and notations, the ratio of uranium and total areas is

$$\frac{A_U}{A_V} = \frac{1+S_U}{1+S_V} \cdot \frac{S_V - S_R}{S_U - S_R} \qquad (7)$$

This is the main formula for radon correction. Here S_U and S_R are some “calibration constants”, for fields of pure sources – only uranium U or only radon Rn. Values of A_V and S_V are directly measured in spectra. Value of A_U is the photopeak area without radon, i.e. it is radon corrected. As can be seen, (7) is interpolation formula: A_V is a combination of A_U and A_R with their S_U and S_R. The graph of A_U/A_V from S_V with S_U=4.0 and S_R=1.0 is in Fig.6.

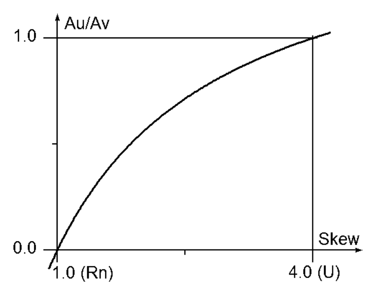

Fig. 6. Interpolation for S_V according to (7).

One shortcoming is that some “calibration” parameters S_U and S_R are required, which are not determined too accurately. By experience, in cases where sensors with volumes of 48L and 32L were used (which implies shorter distances of averaging), it turned out that quite satisfactory results are obtained with S_U equal to about 3.5-4.0 and S_R equal to about 1.0-1.5. Hence, it can be assumed that the “constants” S_U and S_R are not very dependent on the flight height and other survey conditions.

Another shortcoming is that the measured values of A_V and S_V, given the restrictions on averaging distances, remain quite noisy. In particular, the value of S_V, which in the model should lie between S_R and S_U, often does not fall into the interval (1, 4).

There are so far two ways to deal with these noises. First, values of S_V can be forced into the range (S_R, S_U), e.g. using a (broken approximation of) sigmoid function. The second method is to extend the range (S_R, S_U) to approximately the measured values of skew S_V. Usually, the second method gives more acceptable results with quantiles of about 5% of S_V to set values (S_R, S_U).

In addition, this correction can be made in grids, with a somewhat reduced range of values and, moreover, interactive selection on trial grids of moderate sizes is possible.

Examples

The Skew parameter for the radon correction is computed by averaging along the lines, so it inevitably has a noticeable levelling problems or herringbone effects (Whitehead and Musselman, 2006). For the described survey, to make the radon correction in grids, first the herringbone effects were suppressed, then radon correction was done.

The example below is for 1.76 band. Statistics of Skew parameters for 1.76 and 1.46 in grids are shown in Table 4 (see Press et al., 2007 for definitions of statistics).

Table 4. Statistics of 1.46 and 1.76 bands for their Skew fields in grids.

Grid	Min	Max	Mean	Standard	Kurtosis
1.46	0.28	3.5	0.49	0.13	149
1.76	0.01	11.2	1.45	1.01	5.1

It is important that the standard for 1.46 band is much less than for 1.76 band, and the kurtosis for 1.46 band is much more than for 1.76 band. This means that the actual distribution of Skew for 1.46 is almost delta-shaped, and as for radon correction it is almost equivalent to a constant, without leading to informative changes.

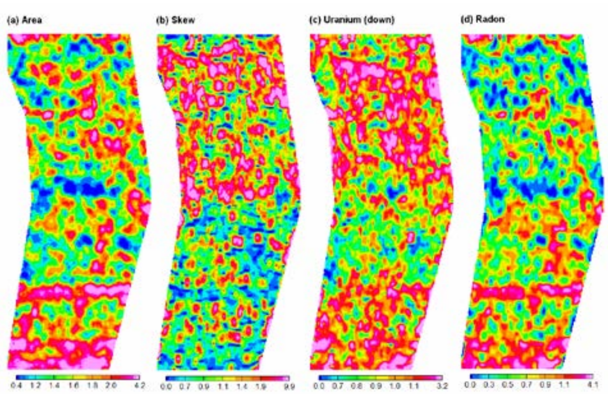

Fig. 7. Example of radon correction for 1.76 band. Maps, left to right: (a) Area; (b) Skew; (c) uranium "down", radon corrected; (d) radon.

In the example, it is clear that the radon correction led to a more believable behavior of the fields of uranium and radon. The same transformation for 1.12 gave pretty similar maps. But similar transformations for 1.46 and 2.61 led to a simple splitting of the original field into two almost identical, without giving any new information.

Results

The proposed procedure of radon correction does not imply any particularities in the distribution of radon (e.g., uniformity or inverse layer). In a sense, this radon correction can be considered as a special case of predictive modeling, since it is a variant of elementary statistical analytics that uses historical and current data to produce a result.

The procedure for radon correction consists of the following main steps:

1. Smooth or average the spectra along the lines and along the energies. The smoothing along the lines must be consistent with the distance of influence of the field sources, otherwise it affects the scale of the measurements. It should also be consistent with the noises in spectra and spectrometer resolution. Naturally, such smoothing leads to the selected direction along the lines, and noticeable noises still remain.

2. Calculate the parameters of Area and Skew at each point where this is possible, even if only formally. Interpolate and smooth to reduce noises.

3. Select the calibration parameters S_R and S_U, e.g. as quantiles of the empirical distribution. Generally speaking, the calibration parameters themselves are unlikely to change depending on the area of the survey and its geology, or on the time of the survey, and therefore can be considered as constants for the spectrometer. Needless to say, any statistic values depend on the parameters of averaging, interpolation, smoothing, etc.

4. Make the radon correction. This can be done both in lines and in grids, which have been previously cleared from herringbone pattern. In the transition to grids, there is some ambiguity: the simultaneity of measurements which are taken into account in the current grid node is lost just due to interpolation between lines. Here is an example for the survey. Typical speed differences between adjacent lines of a flight are 2 m/s, sometimes reaching 5 m/s. With an average line duration of 360 seconds, the changing configuration of radon sources moves by 700 m and more (considering only the speed along the lines), i.e. farther than 3*MFP. So at the nearest point of the adjacent line the spectrometer enters another radon field. It remains to believe that changes in the configuration and location of radon sources do not affect the measured spectra too much.

In this regard, it is interesting to note that there were a few cases when the radon map was of some geological meaning, since the successful confluence of meteorological circumstances led to the mapping of places where radon leaked from the ground more intensely than from others.

Conclusions

A new method for radon correction in AGRS data was proposed. The method is based on measurable parameters of the spectra and does not rely on the special features of the gamma radiation and spectra, and it does not use assumptions about the distribution of radon. It is easy to use and gives relatively local and reliable results.

The method is performed in two stages. First stage, computing the method parameters, usually should be done line-by-line. Second stage, making the radon correction, can be done in lines as well as in (corrected for herringbone pattern) grids. The main advantages of the proposed correction is its simplicity and locality.

Thus, a geophysicist now has several methods for radon correction and a problem of choosing between them. To solve the problem, there is a great rule in the spirit of R. Grasty (Gamma-Bob): If a correction corrects the data the correction is correct (what improves the data is true).

References

Bristow Q., 1983. Airborne γ-ray spectrometry in uranium exploration. Principles and current practice. The International Journal of Applied Radiation and Isotopes, 34(1), 199-229.

Chen X., Paatero J., Kerminen V.-M., Riuttanen L., Hatakka J., Hiltunen V., Paasonen P., Hirsikko A., Franchin A., Manninen H.E., Petaja T., Viisanen Y., Kulmala M., 2016. Responses of the atmospheric concentration of radon-222 to the vertical mixing and spatial transportation. Boreal Environment Research, 21(3-4), 299-318.

Druker E., 2018. Airborne gamma-ray spectra processing: Extracting photopeaks. Journal of Environmental Radioactivity, 187, 22-31.

Grasty R. L., Darnley A. G., 1971. The calibration of gamma-ray spectrometers for ground and airborne use. Geological Survey of Canada, 71-17, 32 pp.

Grasty R.L., Minty B.R.S., 1995. A Guide to the Technical Specifications for Airborne Gamma-Ray Surveys, AGSO, Australia, 89 pp.

Grasty R.L., Wilkes P.G., Kooyman R., 1988. Background measurements in gamma-ray surveys. Geological Survey of Canada, 88-11, 31 pp.

Hotzl H., Winkler R., 1993. Rapid determination of radon daughters and of artificial radionuclides in air by online gamma-ray spectrometry. Radiation and Environmental Biophysics, 32, 129-135.

Hovgaard J., Grasty, R.L., 1997. Reducing Statistical Noise in Airborne Gamma-Ray Data Through Spectral Component Analysis. Proceedings of Exploration 97, 753-764.

IAEA, 1979. Gamma-ray surveys in uranium exploration. Tech. Reports Series No. 186. IAEA, Vienna, 104 pp.

IAEA, 1991. Airborne Gamma Ray Spectrometer Surveying. Tech. Reports Series No. 323. IAEA, Vienna, 116 pp.

IAEA, 2003. Guidelines for radioelement mapping using gamma ray spectrometry data. TECDOC-1363. IAEA, Vienna, 179 pp.

IAEA, 2013. Advances in Airborne and Ground Geophysical Methods for Uranium Exploration. NUCLEAR ENERGY SERIES No. NF-T-1.5. Vienna, 72 pp.

Jurza P., Campbell I., Robinson P., Wackerle R., Cunneen P., Pavlik B., 2005. Use of 214Pb photopeaks for Radon removal: utilizing current airborne gamma-ray spectrometer technology and data processing. Exploration Geophysics, 36, 322-328.

Killeen P.G., Mwenifumbo C.J., Ford K.L., 2015. Tools and Techniques: Radiometric Methods. In "Treatise on Geophysics (Second Edition)" edited by G. Schubert, Volume 11: Resources in the Near-Surface Earth, Elsevier B.V., 447–524.

Knoll G.F., 2000. Radiation Detection and Measurement, 3rd edn, John Wiley & Sons, 816 pp.

Minty B.R.S., 1992. Airborne gamma-ray spectrometric background estimation using full spectrum analysis. Geophysics, 57(2), 279-287.

Minty B.R.S., 1998. Multichannel models for the estimation of radon background in airborne gamma-ray spectrometry. Geophysics, 63(6), 1986-1996.

Minty B.R.S., Luyendyk A.P.J., Brodie R.C., 1997. Calibration and data processing for airborne gamma-ray spectrometry. AGSO Journal of Australian Geology & Geophysics, 17(2), 51-62.

Minty B.R.S., McFadden P., Kennett B.L.N., 1998. Multichannel processing for airborne gamma-ray spectrometry. Geophysics, 63(6), 1971-1985.

Nelson G., Reilly D., 1990. Gamma-Ray Interactions with Matter. LANL Research Library LWW Project, 16 pp.

Press W.H., Teukolsky S.A., Vetterling W.T., Flannery B.P., 2007. Numerical recipes: The art of scientific computing. 3rd edn, Cambridge University Press, 1256 pp.

Schwarz G.F., Klingele E.E., Rybach L., 1992. How to handle rugged topography in airborne gamma-ray spectrometry surveys. First Break, 10(1), 11-17.

Acknowledgments

I am grateful to Vladimir Kertsman and Sergey Sklovsky (Aerogeophysica, Russia), Gregory Rozenberg (Geophysical Consultant, USA) and Tomas Grand (TGrand Ltd, Slovakia) for their interest in the work, providing the field data and discussions.